3. A. J. Heinrich, C. P. Lutz, J. A. Gupta, D. M. Eigler, *Science* **298**, 1381 (2002).
4. Y. Sugimoto *et al.*, *Nat. Mater.* **4**, 156 (2005).
5. Y. Sugimoto *et al.*, *Phys. Rev. Lett.* **98**, 106104 (2007).
6. M. Ternes, C. Lutz, C. Hirjibehedin, F. Giessibl, A. Heinrich, *Science* **319**, 1066 (2008).
7. O. Paz, I. Brihuega, J. M. Gómez-Rodríguez, J. M. Soler, *Phys. Rev. Lett.* **94**, 056103 (2005).
8. R. D. Piner, J. Zhu, F. Xu, S. Hong, C. A. Mirkin, *Science* **283**, 661 (1999).
9. Materials and methods are available as supporting online material on *Science* Online. In AFM experiments we used the easyPLL Plus (Nanosurf, Liestal, Switzerland) for the detection and regulation of the cantilever dynamics, and data acquisition and representation was performed using a Dulcinea SPM controller (Nanotec Electrónica, Madrid, Spain) (*29*).
10. T. R. Albrecht, P. Grütter, D. Horne, D. Rugar, *J. Appl. Phys.* **69**, 668 (1991).
11. S. T. Jemander, N. Lin, H. M. Zhang, R. I. G. Uhrberg, G. V. Hansson, *Surf. Sci.* **475**, 181 (2001).
12. Y. Sugimoto *et al.*, *Phys. Rev. B* **73**, 205329 (2006).
13. M. A. Lantz *et al.*, *Science* **291**, 2580 (2001).
14. Y. Sugimoto *et al.*, *Nature* **446**, 64 (2007).
15. M. Abe, Y. Sugimoto, O. Custance, S. Morita, *Appl. Phys. Lett.* **87**, 173503 (2005).
16. N. Oyabu *et al.*, *Phys. Rev. Lett.* **96**, 106101 (2006).
17. D. M. Eigler, C. P. Lutz, W. E. Rudger, *Nature* **352**, 600 (1991).
18. P. Jelinek, H. Wang, J. P. Lewis, O. F. Sankey, J. Ortega, *Phys. Rev. B* **71**, 235101 (2005).
19. F. J. Giessibl, *Phys. Rev. B* **56**, 16010 (1997).
20. J. E. Sader, S. P. Jarvis, *Appl. Phys. Lett.* **84**, 1801 (2004).
21. H. Hölscher *et al.*, *Phys. Rev. B* **64**, 075402 (2001).
22. U. Dürig, *Appl. Phys. Lett.* **75**, 433 (1999).
23. N. Sasaki, M. Tsukada, *Jpn. J. Appl. Phys.* **39**, L1334 (2000).
24. L. N. Kantorovich, T. Trevethan, *Phys. Rev. Lett.* **93**, 236102 (2004).
25. G. Mills, H. Jónsson, *Phys. Rev. Lett.* **72**, 1124 (1994).
26. T. Shinada, S. Okamoto, T. Kobayashi, I. Ohdomari, *Nature* **437**, 1128 (2005).
27. B. E. Kane, *Nature* **393**, 133 (1998).
28. D. Kitchen, A. Richardella, J.-M. Tang, M. E. Flatté, A. Yazdani, *Nature* **442**, 436 (2006).
29. I. Horcas *et al.*, *Rev. Sci. Instrum.* **78**, 013705 (2007).

30. S.Y., O.C., M.A., and S.M. acknowledge support from grants in aid for scientific research from the Ministry of Education, Culture, Sports, Science and Technology (MEXT), JST, Handai Frontier Research Center, the Project Atomic Technology funded by MEXT, and Global Center of Excellence program "Center for Electronic Devices Innovation." O.C. also acknowledges support from the Air Force Office of Scientific Research–Asian Office of Aerospace Research and Development. The work of Y.S. is supported by the Frontier Research Base for Global Young Researchers funded by MEXT. P.P. and R.P. acknowledge the support of Ministerio de Educación y Ciencia (Spain) and computer time provided by Red Española de Supercomputación at the Barcelona Supercomputing Center. P.J. acknowledges the support of Grantová Agentura Akademie Věd (Czech Republic)

Supporting Online Material
www.sciencemag.org/cgi/content/full/322/5900/413/DC1
Materials and Methods
Figs. S1 to S8
References

16 May 2008; accepted 9 September 2008
10.1126/science.1160601

Catalytic Conversion of Biomass to Monofunctional Hydrocarbons and Targeted Liquid-Fuel Classes

Edward L. Kunkes, Dante A. Simonetti, Ryan M. West, Juan Carlos Serrano-Ruiz, Christian A. Gärtner, James A. Dumesic*

It is imperative to develop more efficient processes for conversion of biomass to liquid fuels, such that the cost of these fuels would be competitive with the cost of fuels derived from petroleum. We report a catalytic approach for the conversion of carbohydrates to specific classes of hydrocarbons for use as liquid transportation fuels, based on the integration of several flow reactors operated in a cascade mode, where the effluent from the one reactor is simply fed to the next reactor. This approach can be tuned for production of branched hydrocarbons and aromatic compounds in gasoline, or longer-chain, less highly branched hydrocarbons in diesel and jet fuels. The liquid organic effluent from the first flow reactor contains monofunctional compounds, such as alcohols, ketones, carboxylic acids, and heterocycles, that can also be used to provide reactive intermediates for fine chemicals and polymers markets.

Diminishing petroleum reserves and growing concerns about global climate change necessitate the development of fuel production pathways based on renewable resources, such as biomass-derived carbohydrates. The conversion of biomass-derived carbohydrates to liquid transportation fuels requires removal of most, or all, of the oxygen atoms in the reactants to form molecules having desirable properties for combustion. To produce nonoxygenated liquid fuels, this removal of oxygen must be accompanied by isomerization to form branched hydrocarbons for gasoline, and/or by C-C coupling reactions to increase the molecular weight for diesel and jet fuels. We have previously outlined a strategy involving dehydration of sugars (e.g., fructose) over acid catalysts to form furan derivatives (e.g., hydroxymethylfurfural, HMF) that can subsequently undergo aldol condensation with ketones (e.g., acetone), followed by hydrodeoxygenation to form C_9 to C_{15} alkanes for use in diesel and jet fuels (*1*, *2*). Here, we outline a strategy that begins the oxygen-removal process by converting sugars and polyols over a Pt-Re catalyst to form primarily hydrophobic alcohols, ketones, carboxylic acids, and heterocyclic compounds (Fig. 1). This process can be used to produce ketones for C-C coupling with HMF, thereby replacing the acetone in our previous process with ketones derived directly from biomass. This alternative process does not require the separate formation of HMF, because we demonstrate that the ketones produced can undergo self-coupling reactions. In addition, this process provides a route to highly branched alkanes and olefins, as well as alkylated aromatics, these compounds being high-octane components of gasoline (*3*, *4*). Moreover, intermediate compounds formed during the conversion of biomass-derived carbohydrates to liquid transportation fuels can serve as valuable compounds for the chemical and polymer industries.

The conversion of carbohydrates over metal catalysts proceeds via reaction pathways involving C-C and C-O bond scission (*5*, *6*). High rates of C-C cleavage lead to the formation of CO, CO_2, and H_2 (denoted as "reforming"), whereas high rates of C-O cleavage produce alkanes (*5*, *6*). Our approach here is to achieve controlled rates of C-C and C-O cleavage, leading to the formation of monofunctional hydrocarbons. This behavior is analogous to achieving selective hydrogenation of acetylene to ethylene, without undergoing further reaction to form ethane over metal catalysts (*7*), where strongly adsorbed reactants preferentially occupy surface sites compared to more weakly adsorbed reaction intermediates, thus allowing the production of these reaction intermediates with high yield.

In the initial step of our process, a fraction of the polyol or sugar feed is reformed over Pt-Re/C to supply the hydrogen required to partially deoxygenate the remainder of the feed to monofunctional hydrocarbons. Endothermic reforming reactions are balanced with exothermic deoxygenation reactions in the same reactor, such that the overall conversion is mildly exothermic and more than 90% of the energy content of the polyol or sugar feed is retained in the reaction products. As outlined schematically in Fig. 1 for a polyol feed, we propose that reforming reactions involve adsorption and dehydrogenation of the polyol, followed by C-C cleavage, leading to CO adsorbed on the catalyst surface, which reacts with water to produce H_2 and CO_2 by the water–gas shift reaction. (This production of CO_2 is required for the overall conversion of polyols to monofunctional hydrocarbons, because a fraction of the polyol feed must be converted to H_2 and CO_2 to generate the hydrogen required for deoxygenation reactions.) Adsorbed polyol species

---

Department of Chemical and Biological Engineering, University of Wisconsin–Madison, Madison, WI 53706, USA.

*To whom correspondence should be addressed. E-mail: dumesic@engr.wisc.edu

can also undergo C-O bond cleavage to form surface intermediates with lower susceptibility toward reforming reactions and with lower binding energies on the surface, facilitating desorption and resulting in the formation of alcohols and ketones, carboxylic acids (following OH migration analogous to the benzilic acid rearrangement), and heterocyclic compounds (following intramolecular dehydration). These monofunctional hydrocarbons can undergo further conversion to alkanes.

Results from density functional theory calculations suggest that cleavage of C-C bonds on Pt for an oxygenated hydrocarbon takes place through transition states that have lower energy and that are more dehydrogenated compared to transition states for cleavage of C-O bonds (*8*), suggesting that C-O cleavage should be favored versus C-C cleavage by operating at reaction conditions in which the surface is highly covered by strongly adsorbed species, such as adsorbed CO and highly oxygenated reaction intermediates (*8*). Furthermore, Re has been shown to promote the rate of C-O hydrogenolysis reactions for oxygenated hydrocarbons (*9*). Because the binding energies of oxygen atoms and hydroxyl groups are stronger on Re than on Pt (*10*), the effects of Re in Pt-Re/C catalysts may be mediated by the presence of oxygen and/or hydroxyl groups associated with Re atoms on the surface of Pt-Re alloy particles.

The primary biomass-derived reactants addressed in this work are glucose and sorbitol, the latter of which can be formed in nearly 100% yield by hydrogenation of glucose (*11*). Glucose can be derived from the acid hydrolysis of cellulose (*12*), the most abundant carbohydrate found in nature, or obtained more directly from edible crops such as sugar cane (with cellulose being the most desirable long-term source of sugar). We show here that sorbitol and glucose can be converted over a carbon-supported Pt-Re catalyst at temperatures near 500 K to a hydrophobic organic liquid containing alcohols, ketones, carboxylic acids, and alkanes containing four, five, or six carbon atoms, as well as heterocyclic tetrahydrofuran and tetrahydropyran compounds (Fig. 1). Biomass can also be converted to fuels and chemicals by pyrolysis at high temperatures (>770 K) to form a liquid product commonly referred to as "bio-oil," followed by upgrading to naphtha-like products or conversion to synthesis gas or H_2 (*13*, *14*). Whereas bio-oil from pyrolysis is a complex mixture of more than 300 highly oxygenated compounds and can contain up to 50 weight percent (wt %) water (*13*, *14*), the liquid product from catalytic conversion of sorbitol or glucose over Pt-Re/C contains a well-defined mixture of hydrophobic species. Moreover, we have demonstrated additional catalytic processes to convert the carbohydrate-derived organic liquid stream to liquid alkanes, olefins, and/or aromatics with molecular weights and structures appropriate for use as transportation fuels. An advantage of this approach is the removal in the first catalytic step of more than 80% of the oxygen contained in the carbohydrate, allowing subsequent upgrading processes to operate at reduced capacity and with increased efficiency (*15*).

Figure 2 and Table 1 show the effects of temperature, pressure, and space velocity on the selectivities and carbon distributions, respectively, for conversion of a 60 wt % sorbitol in water solution over a 10 wt % Pt-Re (1:1)/C catalyst. Increasing the pressure from 18 to 27 bar at 483 K results in a shift of the effluent carbon from aqueous-phase species to organic-phase species (Table 1). Increasing the pressure at 503 K results in a shift from aqueous-phase species to gaseous species, whereas pressure has a negligible effect at 523 K on the carbon distribution (Table 1). The production of alkanes increases at the expense of oxygenated species as pressure increases at constant temperature, and raising the temperature at constant pressure leads to an increase in the production of alkanes and a decrease in high molecular weight oxygenates (Fig. 2A). An increase in the space velocity from 0.60 to 1.2 hours^{-1} at constant temperature and pressure causes an increase in production of organic-phase species at the expense of gaseous products (Fig. 2B and Table 1), and more specifically, an increase in the yield of ketones, alcohols, and acids, with a concurrent reduction in alkane yield. A further increase of space velocity to 2.4 hours^{-1} shifts the carbon distribution toward aqueous-phase oxygenates. All reaction conditions were tested for at least 24 hours time-on-stream, and the carbon balances closed to within 10%. At 503 K and 18

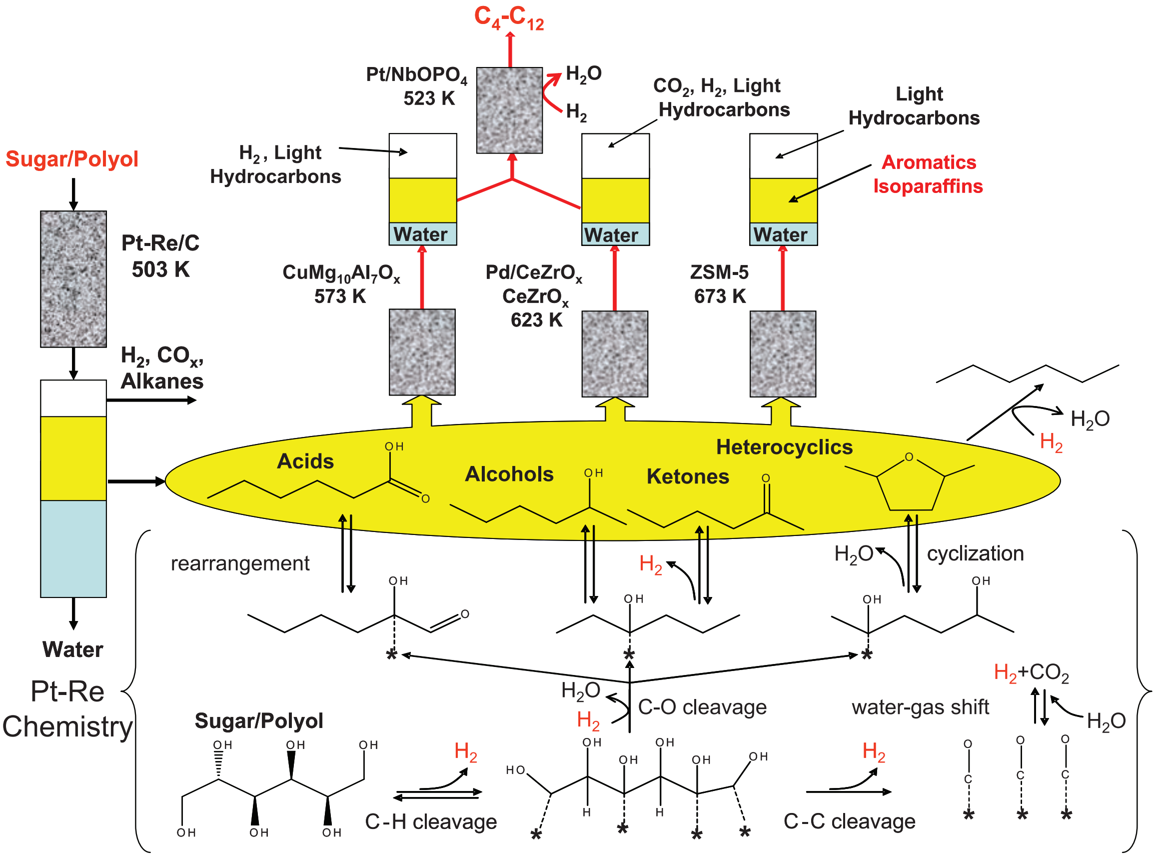

Fig. 1. Schematic representation of reactor sequence used to generate monofunctional organic compounds from catalytic processing of sorbitol or glucose, providing a platform for the production of liquid transportation fuels. The proposed chemistries involved in the conversion of sugars and polyols over Pt-Re catalysts are shown schematically in the lower portion of this figure. The asterisks represent catalytic sites.

bar, Pt-Re/C showed excellent stability for longer than 1 month time-on-stream. This organic liquid product stream, designated as Sorb_503_18, was used for subsequent catalytic processing.

If the rates of reforming and deoxygenation reactions are balanced such that all of the H_2 produced by reforming is utilized by deoxygenated reactions, then the maximum carbon conversion to Sorb_503_18 would be equal to 75%, with the remainder of the carbon being converted to CO_2 (*16*). The actual conversion of the carbon in sorbitol to Sorb_503_18 is 52%, corresponding to a yield of 70% of the maximum value. Deviations from the maximum yield result from the production of CO_2 associated with excess hydrogen, and the formation of gas-phase alkanes. The aforementioned yield corresponds to the production of 1 kg of Sorb_503_18 for every 3.5 kg of sorbitol. If Sorb_503_18 is converted into alkane-based fuels, then these fuels would retain 65% of the energy content of the sorbitol feed (*16*).

We have explored catalytic processes to produce transportation fuel components from the organic liquid effluent produced by conversion of sorbitol over Pt-Re/C (*16*). (The chemistries involved in these catalytic upgrading steps are outlined in the supporting online material.) For example, with respect to gasoline components, we have shown that the organic liquid produced from sorbitol can be converted to aromatic compounds by first hydrogenating the ketones to alcohols (at 433 K and 55 bar H_2 pressure over 5 wt % Ru/C), and then heating to 673 K at atmospheric pressure over H-ZSM-5 (*17*). Of the carbon in the sorbitol-derived organic phase, 25% and 29% is converted to paraffins and olefins containing three and four carbon atoms, respectively, whereas 38% of the carbon is converted to aromatic species (Fig. 3A). Of this aromatic fraction, 12% (5% of total) is converted to benzene, 37% (14% of the total) is converted to toluene, and 30% (11% of the total) is converted to a C_2 benzene (a benzene with two additional carbon atom substituents such as xylenes or ethyl benzene). The remaining 22% of the aromatic fraction (8% of the total) is split between C_3 to C_6 substituted benzene. Overall, 40% of the carbon in the Sorb_503_18 feed is converted into C_{6+} fuel-grade components. In addition, we have shown that gasoline components can be produced by dehydration of secondary pentanols and hexanols (such as the ones present in hydrogenated Sorb_503_18) over an acidic niobia catalyst to form branched C_4 to C_6 olefins, and also by oligomerization of these olefins combined with cracking reactions over H-ZSM-5 to form a distribution of branched olefins centered at C_{12}. The overall process converts 50% of the carbon present in the secondary alcohols into fuel-grade components.

Diesel and jet fuels are composed primarily of hydrocarbons containing carbon atoms linearly arranged to achieve high cetane numbers, whereas gasoline typically contains more highly branched hydrocarbons and aromatic compounds having high octane numbers (*3*, *4*). The heterocyclic compounds present in Sorb_503_18 serve directly as high-octane additives in gasoline (*4*, *18*, *19*). To produce C_8 to C_{12} compounds that contain primarily a single carbon branch and are suitable for conversion to diesel-fuel components, we passed Sorb_503_18 in the presence of H_2 over a bifunctional $CuMg_{10}Al_7O_x$ catalyst to achieve C-C coupling of the C_4 to C_6 ketones and secondary alcohols by aldol condensation [at 573 K and 5 bar pressure with 20 cm^3(STP) min^{-1} H_2 co-feed,

Table 1. Molar carbon distributions (mol %) for the conversion of sorbitol over 10 wt % Pt-Re/C at varying process conditions.

Temperature and pressure study*			
523 K		18 bar	27 bar
% Gas		53	54
% Organic		43	44
% Aqueous		4	2
503 K		18 bar	27 bar
% Gas		36	49
% Organic		52	48
% Aqueous		12	4
483 K		18 bar	27 bar
% Gas		26	30
% Organic		46	57
% Aqueous		29	13
Space velocity study†			
503 K, 27 bar	0.6 $hours^{-1}$	1.2 $hours^{-1}$	2.4 $hours^{-1}$
% Gas	49	33	28
% Organic	48	60	49
% Aqueous	4	7	24

*Three grams of 10 wt % Pt-Re/C catalyst with an atomic Pt:Re ratio of 1:1 was used with a 60 wt % sorbitol feed at a flow rate of 0.04 cm^3 min^{-1} (weight hourly space velocity of 0.6 $hours^{-1}$). †Feed flow rates from 0.04 to 0.16 cm^3 min^{-1} (weight hourly space velocities from 0.6-2.4 $hours^{-1}$) were used with 3.0 g of 10 wt % Pt-Re/C catalyst with an atomic Pt:Re ratio of 1:1.

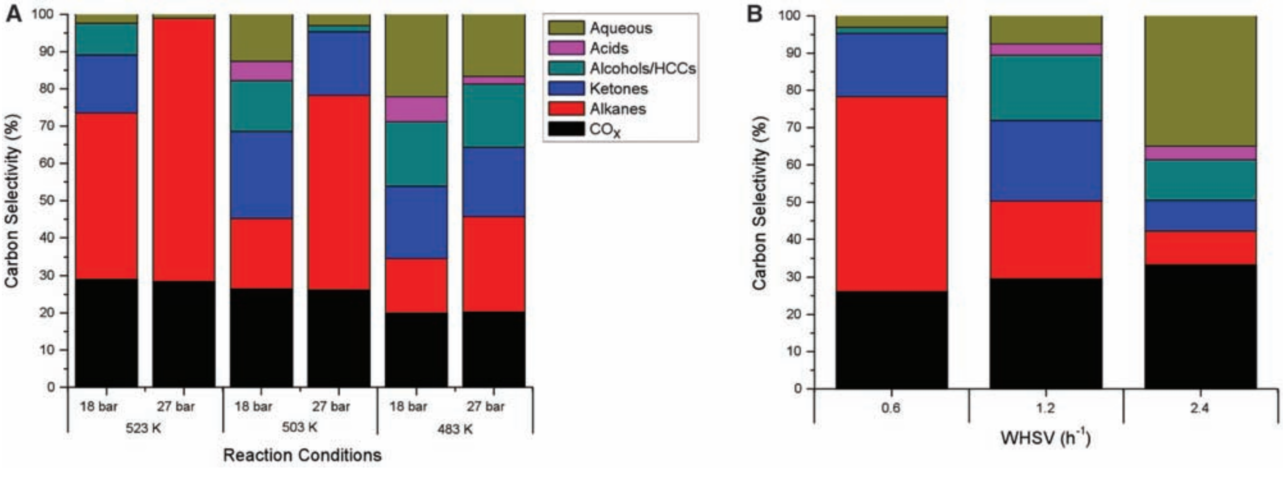

Fig. 2. Carbon selectivities for the conversion of sorbitol over Pt-Re/C. (**A**) Carbon selectivities at pressures between 18 and 27 bar and temperatures between 483 and 523 K. (**B**) Carbon selectivities at feed flow rates between 0.04 and 0.16 cm^3 min^{-1} (weight hourly space velocities between 0.60 and 2.4 $hours^{-1}$) at 27 bar and 503 K. HCCs: heterocyclic hydrocarbon species such as tetrahydrofurans and tetrahydropyrans.

giving a weight hourly space velocity of feed equal to 0.4 hours^{-1}] (*20*, *21*). At these reaction conditions, two-ketones undergo self-aldol condensation or crossed aldol condensation with three-ketones, and primary alcohols are oxidized to aldehydes, which in turn undergo crossed aldol condensation with ketones (*22*, *23*). Self-aldol condensation of three-ketones takes place at a slower rate because of steric and electronic effects (*24*). The small amounts of organic acids and esters in Sorb_503_18 cause deactivation of the basic $Mg_{10}Al_7O_x$ catalyst (*25*). Thus, before condensation, Sorb_503_18 was refluxed with a 20 wt % NaOH solution at 343 K and atmospheric pressure to hydrolyze the esters and neutralize the organic acids.

Figure 3B shows the product distribution following aldol condensation over the $CuMg_{10}Al_7O_x$ catalyst. Light species containing between four and six carbon atoms and one or no oxygen atoms (C_4 to C_6) constitute 55% of the carbon in the products, caused primarily by the low reactivity toward condensation of three-ketones (*26*). These light species contain C_4 alcohols (3% of total carbon) and heterocyclic compounds (substituted tetrahydrofurans and tetrahydropyrans, constituting 9% of total carbon), which would form C_4 to C_6 alkanes upon hydrodeoxygenation (*27*). The C_5 to C_6 ketones and secondary alcohols contribute 32% of the carbon in the products, whereas hexane and pentane contribute 10% of the carbon. The remaining carbon (45%) is associated with condensation products containing between 8 and 12 carbon atoms and one or no oxygen atoms (C_8 to C_{12}). The condensation products can be converted by hydrodeoxygenation over a $Pt/NbOPO_4$ catalyst to the corresponding alkane products (*27*), leading to a distribution similar to that shown in Fig. 3B. Because of the low oxygen content of the condensation products produced in the aforementioned process, the scale of the subsequent hydrodeoxygenation process is reduced in comparison to our previously reported process involving hydrodeoxygenation of the condensation products of acetone with furfural and HMF. The overall aldol-condensation process transforms 40% of the carbon contained in Sorb_503_18 into C_8 to C_{12} species, and converts 90% of the readily condensable methyl ketones present in the feed.

Ketonization reactions, in which two carboxylic acid molecules react to form a ketone with release of CO_2 and H_2O (*28*), can be performed in lieu of the aforementioned neutralization/ester hydrolysis step, to minimize product loss and the use of nonrenewable reagents (NaOH), and simultaneously to provide an additional pathway for C-C coupling. This approach should be particularly effective when the organic phase derived from the conversion of sugars or polyols is rich in carboxylic acids, as is the case for the conversion of a 40 wt % glucose solution over Pt-Re/C at 483 K and 18 bar, giving rise to production of an organic phase containing 40% of the feed carbon. This organic phase, designated Gluc_483_18, consists of 30% C_4 to C_6 carboxylic acids, with the remainder of the carbon present as ketones, alcohols, and alkanes.

Ketonization of Gluc_483_18 was carried out in a fixed bed flow reactor over a $CeZrO_x$ catalyst (weight hourly space velocity = 0.24 hours^{-1}) at two sets of reaction conditions (temperature/pressure): 648 K/1 bar and 573 K/20 bar. The effluent from the reactor was cooled to room temperature and passed to a gas-liquid separator that operated with a continuous flow of inert sweep gas at 20 cm^3(STP) min^{-1}. The first set of ketonization conditions resulted in a 65% carbon yield to liquid organic products, with the remainder of the carbon present in the vapor phase. The vapor phase consisted of C_4 to C_6 oxygenates (60%) resulting from evaporation, CO_2 (15%) resulting from ketonization, and alkanes and alkenes (25%) resulting from dehydration of alcohols. The second set of conditions was used to decrease evaporation and dehydration of light oxygenates, and it yielded 85% conversion to a liquid organic product stream. Both sets of conditions achieved greater than 98% conversion of the carboxylic acids in the feed to C_7 to C_{11} ketones.

The ketones in ketonized Gluc_483_18 can be coupled by aldol condensation to increase the yield of C_{7+} products. We attempted this aldol-condensation step using a $CuMg_{10}Al_{l7}O_x$ catalyst; however, we observed that trace amounts of acids and esters present in the ketonized Gluc_483_18 cause deactivation of the catalyst over a period of 8 hours. In contrast, we found that a bifunctional catalyst consisting of 0.25 wt % Pd on $CeZrO_x$ is stable at 623 K versus time-on-stream for aldol condensation of the ketonized

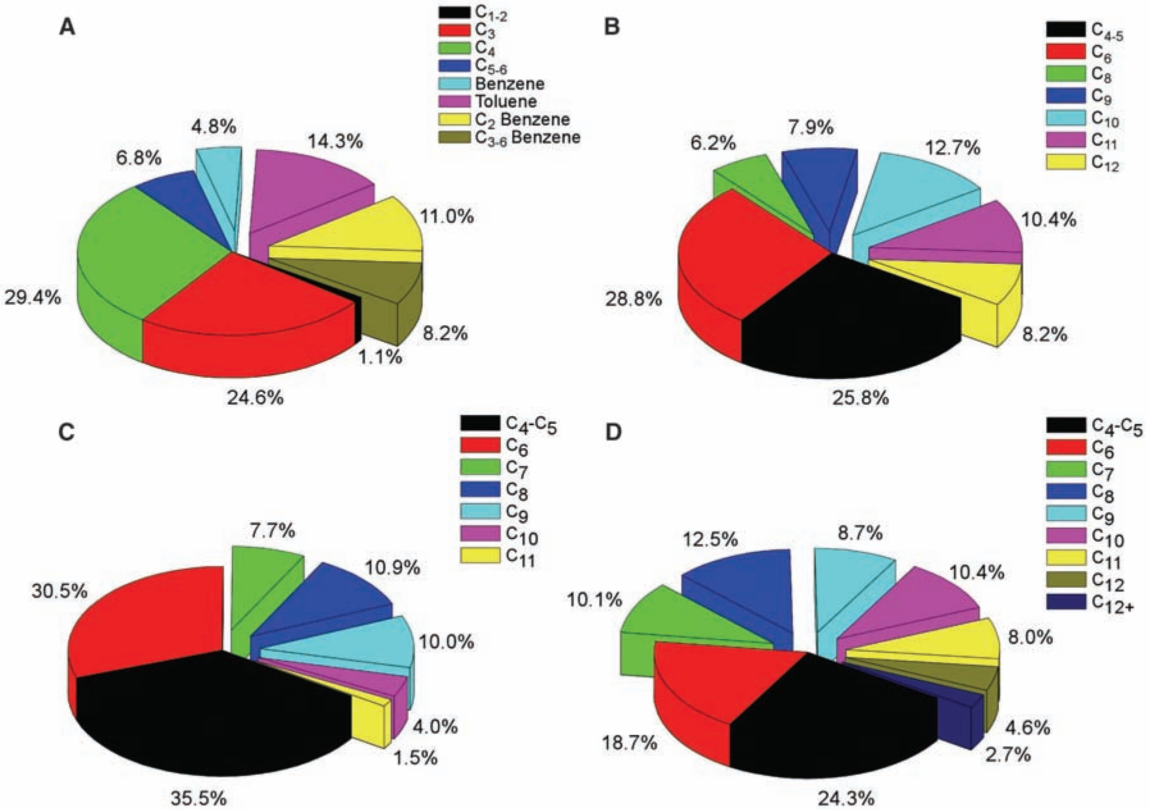

Fig. 3. Product distributions for the upgrading of the organic liquid product from sorbitol or glucose conversion over Pt-Re/C. (**A**) Sorb_503_18 upgrading to olefins and aromatic species over H-ZSM-5 at 673 K and atmospheric pressure. C_x: species containing *x* carbon atoms; C_{1-2}: CO_2, CH_4, C_2H_4, and C_2H_6; C_x Benzene: benzene rings functionalized with *x* additional carbon groups. (**B**) Sorb_503_18 aldol condensation to C_8 to C_{12} species over $CuMg_{10}Al_7O_x$ at 573 K and 5 bar. (**C**) Gluc_483_18 ketonization over $CeZrO_x$. (**D**) Aldol condensation of ketonized Gluc_482_18 over 0.25 wt % $Pd/CeZrO_x$ at 623 K and 5 bar.

Gluc_483_18. The feed used for aldol condensation over the $Pd/CeZrO_x$ catalyst consisted of a mixture of the organic products obtained at the two different sets of ketonization conditions mentioned previously: 34% C_7 to C_{11} ketones and 66% C_4 to C_6 alkanes and oxygenates (Fig. 3C). This ketonized organic feed was then subjected to aldol condensation over $Pd/CeZrO_x$ at 623 K, with all other conditions being the same as those used for the condensation of refluxed Sorb_503_18. Of the total carbon in the liquid organic product stream, 57% is in the form of C_{7+} ketones (Fig. 3D), with 34% resulting from ketonization and 23% resulting from aldol condensation. Products with carbon-chain length greater than C_{12} were also observed, likely resulting from aldol condensation of methyl ketones with C_{7+} ketones formed during ketonization. The combined ketonization and aldol-condensation process completely converted the carboxylic acids found in Gluc_503_18 into C_{7+} ketones, whereas 65% of the readily condensable two-ketones in ketonized Gluc_503_18 were converted to heavy products during the aldol-condensation step. Improving the efficiency of the aldol-condensation step and minimizing evaporation during the ketonization step has the potential to increase the overall conversion of Gluc_50_18 to C_{7+} ketones to $\sim$63%. The comparable operating conditions of the ketonization and aldol-condensation processes should permit the integration of these C-C coupling steps into a two-bed single reactor system.

The cost of producing transportation fuels from ligno-cellulosic biomass is controlled primarily by the costs associated with the processing of biomass to produce the fuel (*29*), making it imperative to develop new processes for the conversion of biomass to liquid fuels that involve a limited number of processing steps (*15*). The catalytic approach shown in Fig. 1 is sufficiently simple that it can be used in a limited number of flow reactors, thus achieving low capital costs, but it is sufficiently flexible that it can be employed to produce a variety of liquid-fuel components. Although we have demonstrated promising yields of monofunctional hydrocarbons from conversion of sorbitol and glucose over Pt-Re/C catalysts, it will be important to understand how the composition of the monofunctional hydrocarbon stream is controlled by the nature of the biomass-derived feed, the catalyst, and the reaction conditions, such that high yields of targeted classes of transportation fuels can be achieved during subsequent catalytic upgrading steps.

References and Notes

1. Y. Roman-Leshkov, J. N. Chheda, J. A. Dumesic, *Science* **312**, 1933 (2006).
2. G. W. Huber, J. N. Chheda, C. J. Barrett, J. A. Dumesic, *Science* **308**, 1446 (2005).
3. C. H. Bartholomew, R. J. Farrauto, *Fundamentals of Industrial Catalytic Processes* (Wiley, Hoboken, NJ, 2006).
4. M. T. Barlow, D. J. H. Smith, D. G. Gordon, in European Patent 82689 A2 (1983).
5. R. R. Davda, J. W. Shabaker, G. W. Huber, R. D. Cortright, J. A. Dumesic, *Appl. Catal. B* **56**, 171 (2005).
6. G. W. Huber, R. D. Cortright, J. A. Dumesic, *Angew. Chem. Int. Ed.* **43**, 1549 (2004).
7. G. C. Bond, P. B. Wells, *J. Catal.* **4**, 211 (1965).
8. R. Alcala, M. Mavrikakis, J. A. Dumesic, *J. Catal.* **218**, 178 (2003).
9. V. Pallassana, M. Neurock, *J. Catal.* **209**, 289 (2002).
10. J. Zhang *et al.*, *J. Am. Chem. Soc.* **127**, 12480 (2005).
11. A. Perrard *et al.*, *Appl. Catal. A* **331**, 100 (2007).
12. D. L. Klass, *Biomass for Renewable Energy; Fuels and Chemicals* (Academic Press, San Diego, 1998).
13. S. Czernik, A. V. Bridgwater, *Energy Fuels* **18**, 590 (2004).
14. A. V. Bridgwater, *Appl. Catal. A* **116**, 5 (1994).
15. A. J. Ragauskas *et al.*, *Science* **311**, 484 (2006).
16. Materials, methods, calculations and detailed reaction schemes are available as supporting material on *Science* Online.
17. A. G. Gayubo, A. T. Aguayo, A. Atutxa, R. Aguado, J. Bilbao, *Ind. Eng. Chem. Res.* **43**, 2610 (2004).
18. D. J. Barratt, J. Lin, U.S. Patent 5,925,152 (1999).
19. T. H. Takizawa, S. A. Shimizu, S. S. Yamada, S. H. Ikebe, S. H. Hara, U.S. Patent 5,925,152 (1994).
20. J. I. Di Cosimo, G. Torres, C. R. Apesteguia, *J. Catal.* **208**, 114 (2002).
21. A. A. Nikolopoulos, B. W. L. Jang, J. J. Spivey, *Appl. Catal. Gen.* **296**, 128 (2005).
22. C. Carlini *et al., J. Mol. Catal. A* **220**, 215 (204).
23. C. S. Cho, *J. Mol. Catal. A* **240**, 55 (2005).
24. J. McMurry, Ed., *Organic Chemistry* (Pacific Grove, CA, ed. 5, 2000), pp. 938–940.
25. J. Lopez, J. Sanchez Valente, J.-M. Clacens, F. Figueras, *J. Catal.* **208**, 30 (2002).
26. S. G. Powell, A. T. Nielsen, *J. Am. Chem. Soc.* **70**, 3627 (1948).
27. R. M. West, Z. Y. Liu, M. Peter, J. A. Dumesic, *ChemSusChem* **1**, 417 (2008).
28. O. Nagashima, S. Sato, R. Takahashi, T. Sodesawa, *J. Mol. Catal. A* **227**, 231 (2005).
29. C. N. Hamelinck, A. P. C. Faaij, H. den Uil, H. Boerrigter, *Energy* **29**, 1743 (2004).
30. This work was supported by the U.S. Department of Energy Office of Basic Energy Sciences and the NSF Chemical and Transport Systems Division of the Directorate for Engineering. We thank M. Mavrikakis for valuable discussions throughout this project, and E. I. Gürbüz for help with flow reactor experiments. J.C.S.-R. thanks the Spanish Ministry of Science and Innovation for postdoctoral support; C.A.G. thanks the German Academic Exchange Service (DAAD) for a scholarship. J.A.D. owns founders stock in Virent Energy Systems, a company with interest in the area of this research. The Wisconsin Alumni Research Foundation at University of Wisconsin has applied for a patent based partly on the work described here.

Supporting Online Material

www.sciencemag.org/cgi/content/full/1159210/DC1
Materials and Methods
Fig. S1
Table S1
References

16 April 2008; accepted 5 September 2008
Published online 18 September 2008;
10.1126/science.1159210
Include this information when citing this paper.

Accurate Temperature Imaging Based on Intermolecular Coherences in Magnetic Resonance

Gigi Galiana,[1,2] Rosa T. Branca,[2] Elizabeth R. Jenista,[2] Warren S. Warren[2]*

Conventional magnetic resonance methods that provide interior temperature profiles, which find use in clinical applications such as hyperthermic therapy, can develop inaccuracies caused by the inherently inhomogeneous magnetic field within tissues or by probe dynamics, and work poorly in important applications such as fatty tissues. We present a magnetic resonance method that is suitable for imaging temperature in a wide range of environments. It uses the inherently sharp resonances of intermolecular zero-quantum coherences, in this case flipping up a water spin while flipping down a nearby fat spin. We show that this method can rapidly and accurately assign temperatures in vivo on an absolute scale.

Temperature, one of the most fundamental intrinsic quantities of matter, is very difficult to measure noninvasively beneath the surface of an object. A general method to image interior temperatures in soft matter could find a wide range of experimental applications in fields ranging from bulk catalysis and process chemistry to clinical treatment. In medicine alone, temperature distributions in the body have been linked to the critical regulation of metabolism, immune function, and longevity. (*1*) Hyperthermic cancer treatments and radiation therapy are used to kill cancer cells at different stages of growth (*2*–*7*), and numerous groups have developed thermally sensitive formulations (e.g., liposomes) that release drugs selectively within a heated region (*8*–*11*). In practice, however, the utility of all of this work is compromised by the difficulty of accurate temperature imaging in vivo. (*12*) In general, current methods break down in the very systems that are of greatest interest, those that are inhomogeneous and that change with time.

Here, we present a magnetic resonance imaging approach for rapid, high-resolution in vivo temperature imaging. It involves selective detection of intermolecular multiple quantum coherences (iMQCs), (*13*–*21*) which in this case correspond to exciting water spin resonances while simultaneously de-exciting lipid resonances from molecules that are separated by the "correlation distance,"

---

[1] Department of Chemistry, Princeton University, Princeton, NJ 08544, USA. [2] Center for Molecular and Biomolecular Imaging, Duke University, Durham, NC 27708, USA.

*To whom correspondence should be addressed. E-mail: warren.warren@duke.edu